Inorganic Chemistry

Article

pubs.acs.org/IC

Monomerizing Alkali-Metal 3,5-Dimethylbenzyl Salts with Tris(*N*,*N*-dimethyl-2-aminoethyl)amine (Me_6TREN): Structural and Bonding Implications

David R. Armstrong,[†] Matthew G. Davidson,[‡] Daniel Garcia-Vivo,[‡] Alan R. Kennedy,[†] Robert E. Mulvey,[†] and Stuart D. Robertson*[,†]

[†]WestCHEM, Department of Pure and Applied Chemistry, University of Strathclyde, 295 Cathedral Street, Glasgow G1 1XL, U.K.
[‡]Department of Chemistry, University of Bath, Bath BA2 7AY, U.K.

Supporting Information

ABSTRACT: The series of alkali-metal (Li, Na, K) complexes of the substituted benzyl anion 3,5-dimethylbenzyl ($Me_2C_6H_3CH_2^-$) derived from 1,3,5-trimethylbenzene (mesitylene) have been coerced into monomeric forms by supporting them with the tripodal tetradentate Lewis donor tris(*N*,*N*-dimethyl-2-aminoethyl)amine, [$N(CH_2CH_2NMe_2)_3$, Me_6TREN]. Molecular structure analysis by X-ray crystallography establishes that the cation−anion interaction varies as a function of the alkali-metal, with the carbanion binding to lithium mainly in a σ fashion, to potassium mainly in a π fashion, with the interaction toward sodium being intermediate between these two extremes. This distinction is due to the heavier alkali-metal forcing and using the delocalization of negative charge into the aromatic ring to gain a higher coordination number in accordance with its size. Me_6TREN binds the metal in a η^4 mode at all times. This coordination isomerism is shown by multinuclear NMR spectroscopy to also extend to the structures in solution and is further supported by density functional theory (DFT) calculations on model systems. A Me_6TREN stabilized benzyl potassium complex has been used to prepare a mixed-metal ate complex by a cocomplexation reaction with tBu_2Zn, with the benzyl ligand acting as an unusual ditopic σ/π bridging ligand between the two metals, and with the small zinc atom relocalizing the negative charge back on to the lateral CH_2 arm to give a complex best described as a contacted ion pair potassium zincate.

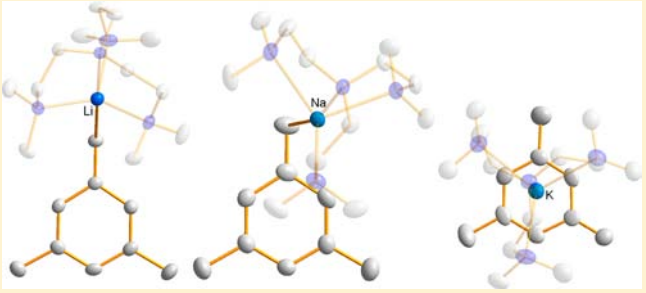

INTRODUCTION

Diversity of aggregation is a defining feature of organo alkali-metal chemistry and is dependent on the identity of both the alkali-metal and the organo-anion. The understanding of aggregation state allows one to rationalize rates of reactivity since there is a strong correlation between the two.[1] The most obvious example is that *t*BuLi is more reactive than *n*BuLi in hydrocarbon solvents because the former is predominantly a tetramer; while the latter is predominantly a hexamer in this Lewis donor free medium.[2] Solvation of transition states may also play a critical role in this reaction rate modification.[3] Therefore, given the pervasive nature of organo alkali-metal reagents throughout synthetic chemistry, it is highly important to understand aggregation as a prelude to understanding reactivity. This rich diversity is of course increased when a third factor is introduced, namely, the presence of a Lewis basic neutral coligand. These tend to be simple molecules such as commercially available ethers (e.g., diethyl ether, Et_2O; tetrahydrofuran, THF; dimethoxyethane, DME) or amines (e.g., *N*,*N*,*N*′,*N*′-tetramethylethylenediamine, TMEDA) which have the effect of deaggregating the organo alkali-metal reagent, with the typical knock-on action being an increase in reactivity.

Recently, we have been drawn to the use of coordinately flexible tris(*N*,*N*-dimethyl-2-aminoethyl)amine (Me_6TREN, Figure 1)[4] as a useful bonding probe in organo alkali-metal chemistry since this tripodal tetra-amine[5] can effectively shield an entire hemisphere of the alkali-metal, leaving only a small coordination arc through which it can interact with a charge neutralizing organoanion.[6]

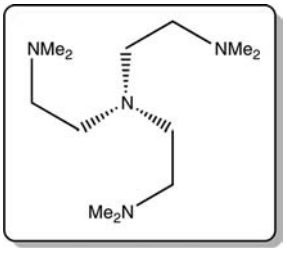

Figure 1. ChemDraw representation of Me_6TREN.

Received: July 16, 2013
Published: October 2, 2013

   dx.doi.org/10.1021/ic401777x | *Inorg. Chem.* 2013, 52, 12023−12032

This generally encourages the formation of highly reactive monomeric species, since the blocking of the potential bonding sites of the alkali-metal from the organoanion prevents the formation of the three-center-two-electron (electron deficient) bonds which propagate oligomerization. This simple way of designing a monomer thus inhibits all secondary bonding and gives an unequivocal view of the primary cation−anion bonding interaction which is taking place. We recently displayed this principle in practice with the preparation of the monomeric series $PhCH_2M{\cdot}Me_6TREN$ (M = Li, **1**; Na, **2**; K, **3**) which showed that the localizing effect of the alkali-metal on the negative charge is gradually diminished as the alkali-metal size is increased; that is the M-anion bonding changes from mainly σ (sp^3 CH_2) to mainly π (sp^2 CH_2) on going from small Li to large K.[7] By studying the bonding picture in the potassium example **3** it could be surmised that the secondary interaction in the polymeric structure of the related complex $[PhCH_2K{\cdot}PMDETA]_\infty$ (Figure 2) is in fact the σ-bond between the CH_2 arm and K rather than the π-bond between the aromatic ring and the metal.[8]

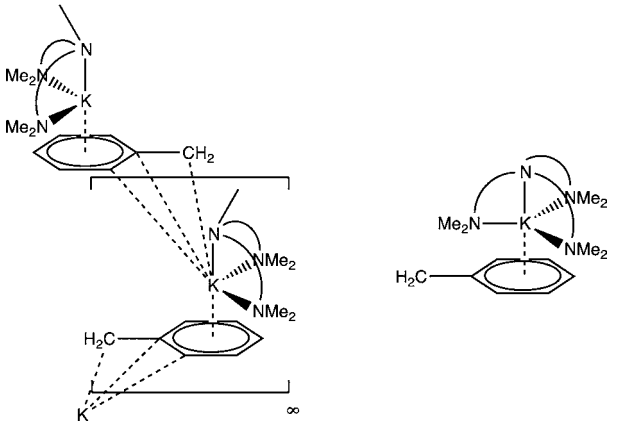

Figure 2. ChemDraw representation of molecular structures of $[PhCH_2K{\cdot}PMDETA]_\infty$ (left) and $PhCH_2K{\cdot}Me_6TREN$ (**3**) monomer (right). CH_2−CH_2 bridges have been simplified to a curved line for clarity.

Reported in a communication, this series of benzyl complexes also represented somewhat of a landmark in alkali-metal chemistry in that the three complexes all contained the same anion, donor, and aggregation state, which up until that point had proved impossible because of the significant differences in ionic radii of the alkali-metals (which tends to result in either different aggregation states and/or different numbers of solvating ligands being involved). Following on from this initial discovery, in this full paper we have taken these studies further to investigate if the above bonding situation was a unique case or whether it could be extended into more challenging substituted benzylic alkali-metal systems. Furthermore we have probed our findings via density functional theory (DFT) calculations which show excellent agreement with the experimental outcomes.

RESULTS AND DISCUSSION

Synthesis of Me_2Bn Alkali-Metal Me_6TREN Monomers. Synthetically we commenced by preparing complexes of general formula $Me_2BnM{\cdot}Me_6TREN$ (M = Li, **4**; Na, **5**; K, **6**; Me_2Bn = 3,5-dimethylbenzyl, C_9H_{11}; see eq 1 for details) in an effort to ascertain whether the benzyl complexes mentioned earlier were

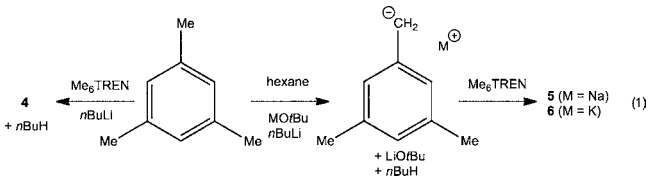

a special case or if the bonding seen previously in complexes **1**−**3** can be considered as representative of benzylic alkali-metal monomers in general. For the lithium complex, a direct deprotonation method was employed whereby *n*BuLi was simply added to a solution of Me_6TREN in bulk mesitylene (1,3,5-trimethylbenzene) with the colorless solution immediately turning orange.[9] For its heavier congeners, a Lochmann−Schlosser approach[10] was taken with the insoluble Me_2BnM solid prepared by introducing *n*BuLi to a hexane solution containing mesitylene and the appropriate heavier alkali-metal *t*-butoxide MO*t*Bu (M = Na, K). The resulting orange or red colored powder was filtered, washed with hexane to remove soluble LiO*t*Bu, and dried under reduced pressure. The powder was subsequently suspended in mesitylene and two molar equivalents of Me_6TREN were then added via syringe to give an intensely colored solution.

All solutions yielded X-ray quality crystalline material upon cooling to −30 °C. The molecular structures were thus determined (see Figures 3−5: with pertinent bond parameters

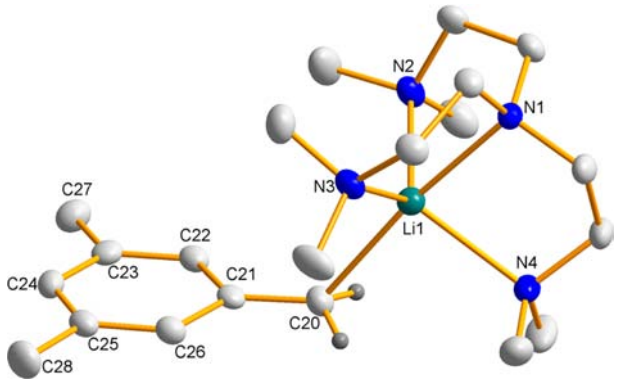

Figure 3. Molecular structure of $Me_2BnLi{\cdot}Me_6TREN$ (**4**). Ellipsoids are displayed at 50% probability, and all hydrogen atoms except those of the metal-CH_2 group are omitted for clarity.

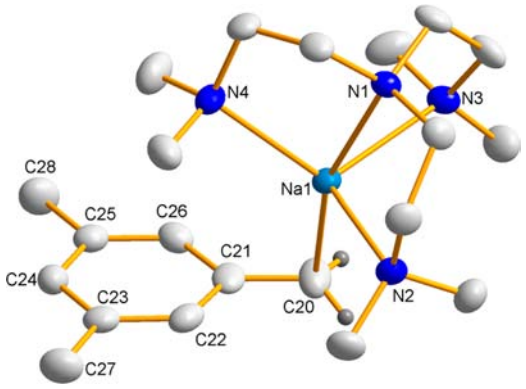

Figure 4. Molecular structure of $Me_2BnNa{\cdot}Me_6TREN$ (**5**). Ellipsoids are displayed at 50% probability, and all hydrogen atoms except those of the metal-CH_2 group are omitted for clarity.

dx.doi.org/10.1021/ic401777x | *Inorg. Chem.* 2013, 52, 12023−12032

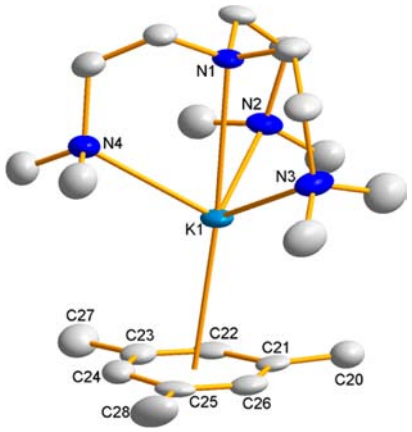

Figure 5. Molecular structure of $Me_2BnK{\cdot}Me_6TREN$ (**6**). Ellipsoids are displayed at 50% probability, and all hydrogen atoms are omitted for clarity.

contained within Table 1) and clearly revealed that bonding between cation and anion in these monomeric complexes is highly dependent upon the identity of the alkali-metal. Geometrically this is most easily discerned by the $C_{ipso}-CH_2-M$ bond angle (C21−C20−M1 in Figures 3−5, with the "metalated" carbon C20 in **6** being simply identified by its C−C bond length as the pair of hydrogen atoms on it could not be located and refined in the molecular structure determination).

It is clear within complexes **4**−**6** that as the size of the alkali-metal increases, the metal migrates from being predominantly σ-bound to the CH_2 appendage (M = Li, **4**) to being predominantly π-bound to the aromatic ring system (M = K, **6**). The sodium structure (**5**) is intermediate between these two extremes, highlighted by the change in angle at the "metalated" carbon atom [C21−C20−M1 = 128.85(10)° in **4**, 90.41(10)° in **5**]. This pattern fits well with the general demarcation in organometallic chemistry with Li and the K/Rb/Cs trio being distinct from each other and Na fluctuating either side of this line of demarcation.[11] These results suggest that as group 1 is descended, the negative charge is delocalized into the aromatic ring with the CH_2 group gaining more sp^2 character. Crystallographically, this is further supported by the $C_{ipso}-CH_2$ bond, which shortens gradually as the metal is changed from Li [1.412(2) Å] through Na [1.405(2) Å] to K [1.388(4) Å].

The transition from a localized negative charge in a benzylic type anion to a delocalized negative charge is typically accompanied by a deformation of the aromatic ring. In particular the $C_{ipso}-C_{ortho}$ and $C_{meta}-C_{para}$ bonds are elongated and the $C_{ortho}-C_{meta}$ bonds are shortened from the ideal aromatic length of 1.4 Å for aromatic C−C bonds, as explained previously by Feil and Harder.[12] While the extent of this deformation noticeably increased moving through the series **1**−**3**, it is not particularly evident in **4**−**6** (Figure 6). This must be a consequence of the additional electron releasing Me substituents at the *meta* positions, which reduce deformation of the aromatic ring caused by the resonance delocalization. However, this smaller electronic perturbation within the carbon framework does not impede the potassium, and to a lesser extent the sodium from taking up steric positions that maximize their coordination numbers in line with their sizes.

The similarity of the aromatic ring bond parameters in complexes **4**−**6** is unsurprisingly repeated in their highest occupied molecular orbital (HOMO) and lowest unoccupied molecular orbitals (LUMOs) (Figure 11, see calculation section for full details).

Interestingly, complex **4** is considerably removed from the only previous 3,5-dimethylbenzyl alkali-metal complex to be characterized crystallographically. With the only distinction being the identity of the polydentate amine donor (in this case bidentate TMEDA - *N*,*N*,*N*′,*N*′-tetramethylethylenediamine), the previously reported complex $[(TMEDA)_2Li]^+[(Me_2Bn)_2Li{\cdot}TMEDA]^-$ adopts a solvent separated lithium lithiate structure, in which a lithium atom resides in both cationic and anionic moieties (Figure 7).[13]

The two dimethylbenzyl ligands in this lithiate display noticeably different bonding to the lithium center. The first can almost be considered as being η^2 bound, with the $Li-C_\alpha$ and $Li-C_{ipso}$ distances of 2.257(2) and 2.637(6) Å (giving a ratio of 1.17, similar to that seen in our Na complex **5**, 1.14) and a $Li-C_\alpha-C_{ipso}$ angle of 89.0(3)°. Meanwhile, the second ligand displays parameters more in line with those of lithium complex **4**, specifically $Li-C_\alpha$ and $Li-C_{ipso}$ bond lengths of 2.325(7) and 3.375(6) Å (ratio 1.45) and a $Li-C_\alpha-C_{ipso}$ angle of 127.8(3)° [c.f. **4**, $Li-C_\alpha$, 2.388(2); $Li-C_{ipso}$, 3.453(2) Å; ratio 1.45; $Li-C_\alpha-C_{ipso}$, 128.85(10)°] and can thus be unequivocally assigned as being η^1 bound.

Power has reported the THF solvated mesityl (isomeric with our anion) lithium cyclo-dimeric complex $(LiMes{\cdot}2THF)_2$;[14] however in this the metal is bound to a ring carbon rather than

Table 1. Selected Bond Parameters for Experimental Me_6TREN Complexes 3−6 and 3·Zn*t*Bu_2 and Their DFT Models

	4	$\mathbf{4}_{calc}$	**5**	$\mathbf{5}_{calc}$	**6**	$\mathbf{6}_{calc}$	**3**·$ZntBu_2$	**3**·$ZntBu_{2calc}$	**3**[7]
M1−C20	2.388(2)	*2.215*	2.568(2)	*2.526*	3.627(3)	*3.405*	3.767(4)	*3.684*	3.893(4)
M1−C21	3.453(2)	*3.136*	2.936(2)	*3.008*	2.954(2)	*2.888*	3.044(3)	*3.010*	3.098(4)
M1−C21/M1−C20	1.45	*1.42*	1.14	*1.19*	0.81	*0.85*	0.81	*0.82*	0.80
C20−C21	1.412(2)	*1.446*	1.405(2)	*1.429*	1.388(4)	*1.390*	1.469(5)	*1.438*	1.390(6)
M1−N1	2.302(2)	*2.457*	2.542(1)	*2.647*	2.953(2)	*3.092*	2.848(2)	*2.974*	2.919(3)
M1−N2	2.191(2)	*2.334*	2.524(1)	*2.564*	2.786(2)	*2.920*	2.798(3)	*2.913*	2.838(3)
M1−N3	2.181(2)	*2.301*	2.524(2)	*2.590*	2.781(3)	*2.938*	2.826(3)	*2.927*	2.822(3)
M1−N4	2.288(2)	*2.457*	2.480(1)	*2.613*	2.802(2)	*2.952*	2.806(3)	*2.927*	2.815(3)
M1−C20−C21	128.85(10)	*116.3*	90.41(10)	*95.0*	50.88(14)	*56.8*	50.09(16)	*51.6*	46.2(2)
K−Ar					2.798(1)		2.868(1)		2.830(1)
Zn1−C20							2.109(4)	*2.220*	
Zn1−C13							2.044(3)	*2.042*	
Zn1−C27							2.045(3)	*2.048*	

dx.doi.org/10.1021/ic401777x | *Inorg. Chem.* 2013, 52, 12023−12032

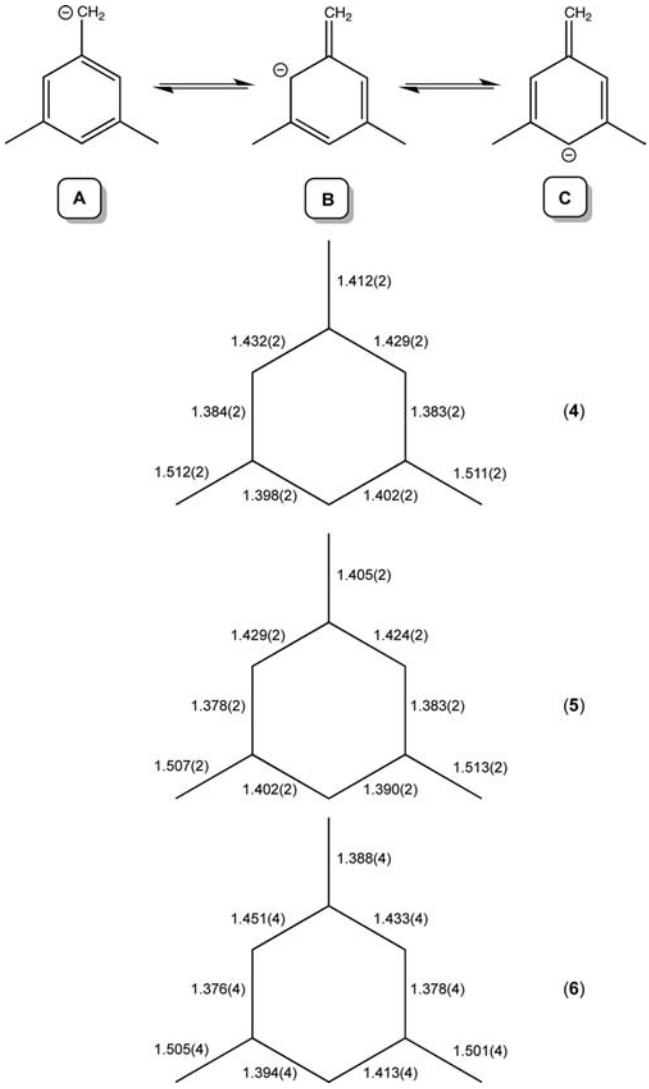

Figure 6. Resonance forms for the anion in complexes **4**–**6** (top) and their C–C bond lengths (in Å) (below).

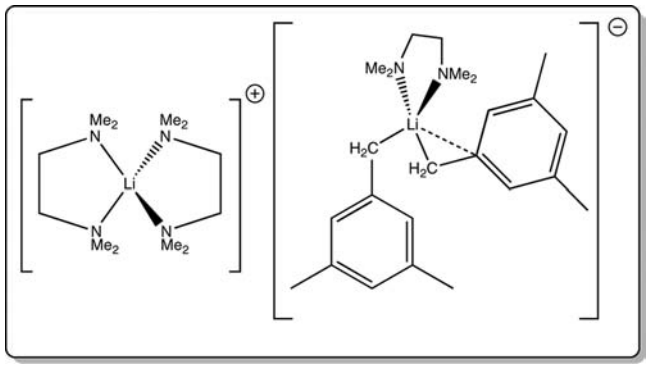

Figure 7. ChemDraw representation of molecular structure of $[(TMEDA)_2Li]^+[(Me_2Bn)_2Li{\cdot}TMEDA]^-$.

a lateral one, giving such a structure more in common with substituted phenyl complexes rather than substituted benzyl complexes as described herein (see Figure 8). We note for completeness that Lerner et al. have reported the molecular structure of unsolvated MesLi as a "polymer of dimers", propagating through η^6 interactions between the Lewis acidic

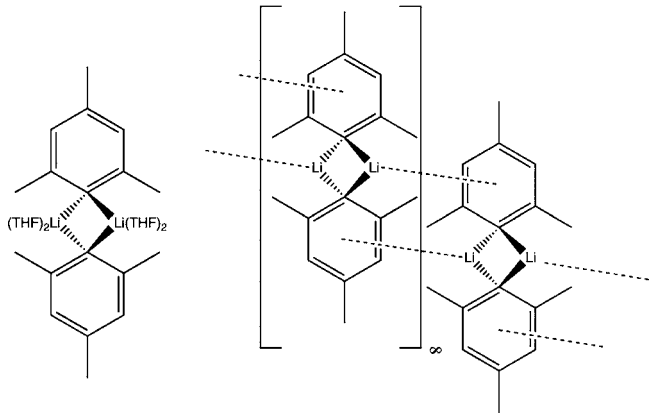

Figure 8. ChemDraw representations of molecular structures of THF solvated LiMes dimer (left) and unsolvated polymer of dimers (right).

lithium centers and the π system of an adjacent mesityl ring as shown above.[15] Also, Davies has reported an excellent series of papers applying the mesityl lithium moiety within a bimetallic Li/Cu framework, although again the metal–carbon contact is through a ring carbon (to copper) with Li binding to the π face of the mesityl anion.[16] Specifically in $Cu_2Li_2(Mes)_2(NBn_2)_2$, η^6 binding, similar to our K based complexes **3** and **6** is seen. Meanwhile, in $Cu_3Li(Mes)_4$ the binding is η^6/η^6 to an aryl ring above and below the metal with the metal lying above the center of the ring while in $Cu_2Li_2(Mes)_4$ a more "slipped" arrangement occurs with a η^6/η^1 bonding mode in place (that is with the *ipso* carbon of the second ring lying directly below the lithium atom).

On perusing bond parameters of other crystallographically characterized alkali-metal benzyl complexes[17] it is discernible that there is a considerable amount of η^2 bonding character in the lithium and sodium complexes described thus far, that is, where the benzyl anion has at least a minor degree of interaction between the *ipso* carbon and the metal, which is expressed most clearly by the C_{ipso}–C_α–M bond angle. Lithium benzyl complexes can be placed in three aggregation categories; namely, monomeric,[18] cyclotetrameric,[18c] and polymeric;[14,19] with sodium congeners also providing cyclotetrameric[20] and polymeric[21] examples.[22] However, regardless of the aggregation state, this C_{ipso}–C_α–M angle tends to deviate no more than 15° from a right angle. While this also holds true for our sodium monomers **2** and **5**, lithium monomers **1** [mean such angle 129.9°] and **4** [128.85(10)°] have a more typical sp^3 type of bonding. We assume this can be ascribed to their greater coordination number (5) as the previously reported monomers each have a coordination number of 4, namely, with THF/TMEDA,[18a] Me_3TACN (*N*,*N*′,*N*″-trimethyl-1,4,7-triazacyclononane)[18b] or PMDETA[18c] acting as the neutral Lewis donor. However, it is worth noting that the Me_6TREN molecule is disposed in such a way that a NMe_2 group does not lie directly above the C_α–C_{ipso} bond, minimizing steric inhibition of a C_{ipso}–Li interaction [smallest C–C–Li–N torsion angles are 53.70(18) and 53.36(15)° for **1** and **4** respectively]. In our sodium monomers **2** and **5**, the C_{ipso}–C_α–M angle has reduced to 103.3(1) and 90.41(10)° respectively, much more indicative of η^2 coordination to the metal. This is despite a NMe_2 group now lying directly above the C–C bond which one would expect would hinder such coordination [smallest C–C–Na–N torsion angles are now 12.56(10) and 16.68(12)° for **2** and **5** respectively]. The longer C–M bond distance presumably thus

dx.doi.org/10.1021/ic401777x | *Inorg. Chem.* 2013, 52, 12023–12032

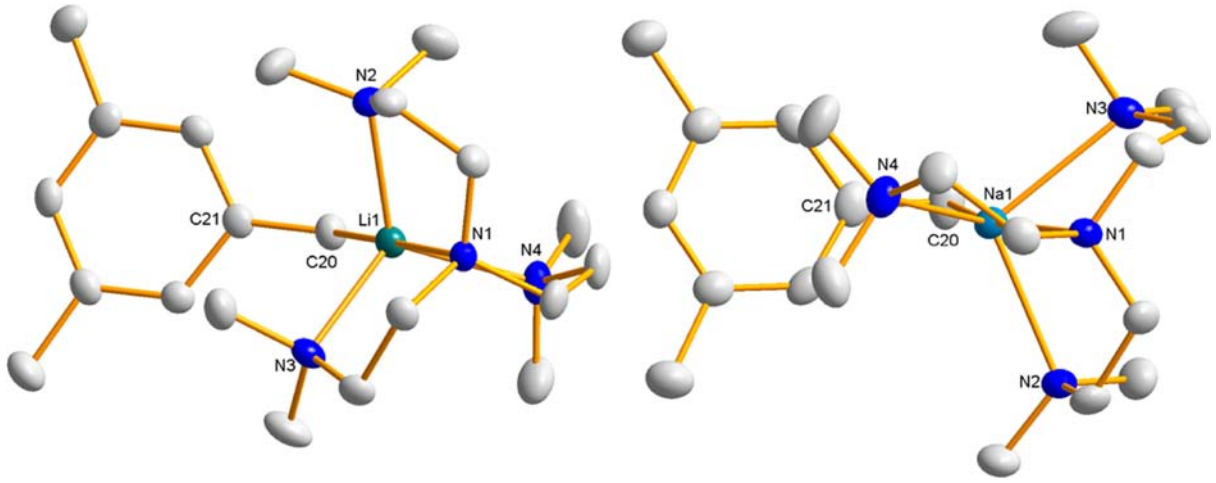

Figure 9. Alternative view of molecular structures of **4** (left) and **5** (right).

plays a role in allowing such a bonding arrangement to take place. A comparison of the Me_6TREN alignments with respect to the mesityl anion of **4** and **5** is shown in Figure 9. There is no obvious reason for the disparity in $C_{ipso}-C_{\alpha}-Na$ angles for **2** and **5**, with the methyl groups an unlikely candidate because of their relatively small bulk and remoteness from the carbanionic center, and it is thus perhaps more likely to be due to a crystal packing effect.

The structural pattern witnessed in the solid state appears to be replicated in solution as evidenced by perusal of ^{1}H NMR data, collected in C_6D_6 solution (summarized in Table 2).

Table 2. Selected ^{1}H NMR Chemical Shift Data (ppm, 400.13 MHz) for Complexes 4−6 in C_6D_6 Solution

	mesitylene	4	5	6	3·Zn*t*Bu$_2$	3[7]
ortho	6.72	6.38	6.21	5.90	7.05	6.16
meta					6.85	6.56
para	6.72	5.83	5.54	4.95	6.29	5.24
CH_2^-	2.16[a]	2.32	2.49	3.27	2.32	3.21
$^1J_{CH}$ (Hz)		133	144	150	127	151

[a] CH_3

The delocalization of the negative charge from the CH_2 arm into the aromatic ring is manifested in the NMR spectrum in two principal ways; the first is the greater shielding of the aromatic proton resonances by the electropositive metal as group 1 is descended and is quite clearly occurring here as demonstrated by the *ortho* and *para* chemical shifts listed in Table 2. The second way is through the C−H coupling of the "metalated" CH_2 arm, which can be discerned either from observing the $^1J(^{13}C-^1H)$ satellites in the ^{1}H NMR spectrum (provided it is in an uncluttered region of the spectrum as they are only 1% intensity) or through collecting a ^{13}C (^{1}H coupled) spectrum. Boche[18a] has previously reported that this coupling constant will be approximately 125 Hz for a perfectly pyramidalized sp^3 system (one with a σ-bound metal such as in **4**) and will rise toward 167 Hz as sp^2 hybridization is approached (that is as in the π bonding situation present in **6**). This sequential increase in the coupling constant is indeed evident, altering from 133 Hz in **4** to 144 Hz in **5** and finally to 150 Hz in **6**. These values are similar to those witnessed for complexes **1**−**3** (131, 142, and 150 Hz, respectively) and suggest that the presence of the extra methyl groups on the aromatic ring have only a negligible effect on the hybridization. The change of hybridization as a function of alkali-metal is further supported by the downfield shift of the CH_2 group resonance away from the alkyl region and toward the olefinic as shown in Table 2. Interestingly, the ^{1}H NMR spectrum of **6** bears little similarity to that of 3,5-dimethylbenzyl potassium in THF (*ortho*, 6.69; *para*, 5.23; methyl, 2.19; CH_2, 1.63 ppm),[23] suggesting that the bonding is considerably different in these complexes.

Kays and co-workers recently reported a pair of lithium carbazol-9-yl complexes. The THF solvated monomer (with no Li-π interactions) gave a ^{7}Li NMR resonance at −1.1 ppm

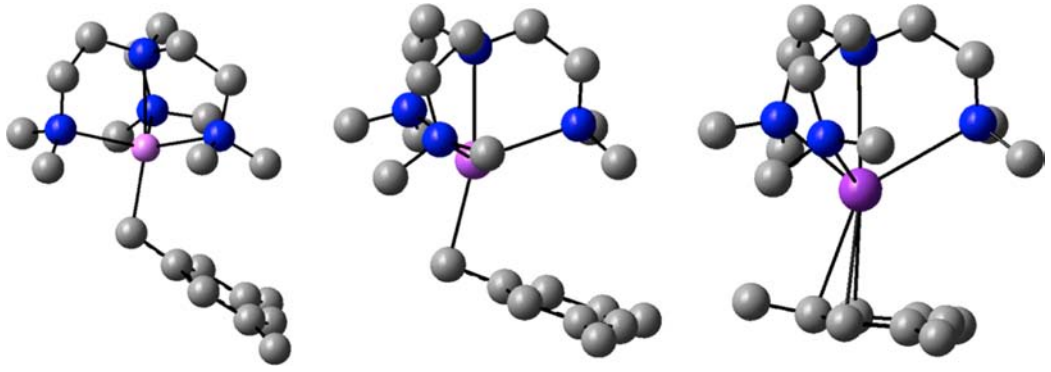

Figure 10. Optimized structures of complexes **4** (M = Li; left), **5** (M = Na; middle), and **6** (M = K; right).

dx.doi.org/10.1021/ic401777x | *Inorg. Chem.* 2013, 52, 12023−12032

while the unsolvated dimer (which dimerizes through a Li-π interaction) gave the corresponding resonance much further upfield at −5.9 ppm because of shielding of the lithium cation by the aromatic π-system.[24] Thus the ^{7}Li NMR resonance of **4** at 0.83 ppm is perhaps indicative that there is no Li-π interaction in solution.

Overall, from the combination of solid state and solution evidence witnessed in these two series we contend that such a pattern of bonding between the alkali-metals and CH_2−Ar anions is probably a general phenomenon in the absence of other structure influencing functional groups.

DFT Calculations. To probe further the coordination isomerism at play in the alkali-metal mesityl complexes **4**−**6** (and indeed the benzyl complexes **1**−**3**) we turned to DFT calculations. The optimized energy minimum structures supported our experimental observations of coordination isomerism with the alkali-metal clearly migrating from being σ bound to the CH_2 group to being π bound to the aromatic ring as the group was descended. These configurations resulted even when the alkali-metal was deliberately forced in the calculation to start in the "wrong" coordination site, that is, with Li binding to the π system of the aryl ring and potassium σ bound to the CH_2 group. The optimized structures of **4**−**6** are displayed in Figure 10 with selected calculated bond parameters in Table 1. Those of **1**−**3** are available in the Supporting Information.

While the bonding trends already witnessed in the experimental structures are essentially replicated in the DFT calculations, the calculations predict a stronger cation−anion interaction and a concomitantly weaker cation-Lewis donor interaction. This is primarily evidenced by the calculated M−CH_2 distances which are all shorter than determined experimentally (by 0.173, 0.042, and 0.222 Å for **4**, **5**, and **6**, respectively), while the M−N_{donor} distances are all predicted to be longer than in complexes **4**−**6** (Table 1). The general trends of the calculated parameters however all mirror those of the experimental molecular structures. Specifically, our calculations suggest that the unique M−N bond (that is the one to the unique central nitrogen atom of Me_6TREN) will be the longest of these in each case, while they also intimate that complex **4** will display a considerable disparity in M−NMe_2 distances (two shorter and one longer) but that the M−NMe_2 bonds will all be similar in complex **5** and also in complex **6**. Further, the structures of $\mathbf{4}_{calc}$ and $\mathbf{5}_{calc}$ confirm the different rotation of the tripodal ligand with respect to the CH_2−C_{ipso} bond, with a staggered arrangement occurring in the lithium example (C−C−Li−N = 40.4°) and approaching a more eclipsed arrangement in the sodium congener (C−C−Na−N = 22.7°).

Next, we considered the atomic charges and bond indices for the series of complexes **1**−**6**. The charge distribution was obtained via a Natural Bond Orbital (NBO) analysis.[25] The results of this (as displayed in Table 3) overwhelmingly corroborated the trends witnessed in the experimentally observed molecular structures. Specifically, we can see that there is a small but significant change in the distribution of charge as the metal is changed from Li to Na and then to K. Unsurprisingly as the group is descended, the positive charge on the metal increases in line with increasing electropositivity from +0.84 (Li) to +0.87 (Na) and to +0.90 (K). However, the negative charge distribution alteration is more pronounced. On moving from Li to Na (which results in only a small movement of the metal as seen by the change in the C−C−M angle, vide supra) the charge on the CH_2 group alters modestly from −0.94 to −0.87. However, on moving to the potassium congener which is considerably removed from the CH_2 arm, the negative charge located here reduces to −0.67. Concomitantly we see an increase in the sum of negative charge on the aromatic carbon atoms as the metal migrates, confirming that the charge is being more delocalized in to the ring. We note in relation to this that Stalke and co-workers showed the localizing effect of a basic heteroatom in their related 2-picolyllithium complexes, which have the negative charge predominantly localized on the *ortho*-nitrogen atom (−1.04) and only −0.19 on the methylene carbon atom.[26]

Table 3. Calculated Atomic Charges and Bond Indices for Complexes 1−6

	1 (M = Li)	**2** (M = Na)	**3** (M = K)	**4** (M = Li)	**5** (M = Na)	**6** (M = K)
M	0.84	0.87	0.90	0.84	0.87	0.90
CH_2	−0.94	−0.87	−0.67	−0.94	−0.87	−0.67
C_{ipso}	−0.02	−0.05	−0.10	0	−0.03	−0.08
C_{ortho}	−0.27	−0.28	−0.31	−0.28	−0.29	−0.33
	−0.28	−0.28	−0.31	−0.29	−0.30	−0.32
C_{meta}	−0.19	−0.20	−0.22	0	0	−0.01
	−0.20	−0.20	−0.22	0	−0.01	−0.01
C_{para}	−0.29	−0.32	−0.39	−0.31	−0.33	−0.40
ΣC_{ring}	−1.25	−1.33	−1.55	−0.88	−0.93	−0.97
M−CH_2	0.06	0.05	0.02	0.06	0.05	0.02
CH_2−C_i	1.27	1.34	1.52	1.27	1.34	1.51
C_i−C_o	1.29	1.26	1.18	1.28	1.25	1.18
	1.29	1.26	1.18	1.29	1.25	1.19
C_o−C_m	1.48	1.5	1.54	1.44	1.46	1.50
	1.48	1.5	1.55	1.46	1.46	1.50
C_m−C_p	1.40	1.38	1.34	1.36	1.35	1.31
	1.40	1.38	1.35	1.37	1.35	1.31

Perusing the bond indices suggests that there is very little covalent bonding character in the M−C bonds, suggesting that the bonding between cation and anion is more ionic (electrostatic) in nature. This effect is most pronounced in the M−CH_2 bond indices which are extremely small (range 0.02−0.06). What is also clear is that the bond index value for the CH_2−C_i bond increases as the metal size increases, in agreement with the fact that this bond decreases in length as the series is crossed. Likewise, the C_i−C_o and C_m−C_p bond indices decrease while those of the C_o−C_m bonds increase, emphasizing the ring deformation which occurs upon charge delocalization as described previously by Harder (vide supra).

We also studied the molecular orbitals of complexes **1**−**6**. Those frontier orbitals of the substituted benzyl derivatives **4**−**6** are displayed in Figure 11 while those of the benzyl complexes **1**−**3** are provided in the Supporting Information. As mentioned earlier, they are essentially the same regardless of the identity of the alkali-metal (and by extension regardless of the mode of cation−anion interaction).

Specifically, the HOMO of each is the highest filled π system of the benzyl anion while the LUMO is located on the Me_6TREN donor which encapsulates the alkali-metal. This similarity would suggest that even though the location of the alkali-metal cation and the location of the negative charge in the anion (localized at the CH_2 or delocalized through the aromatic ring) differs, the seat of reactivity in, for example, an electrophilic quench would result in the electrophile binding

dx.doi.org/10.1021/ic401777x | *Inorg. Chem.* 2013, 52, 12023−12032

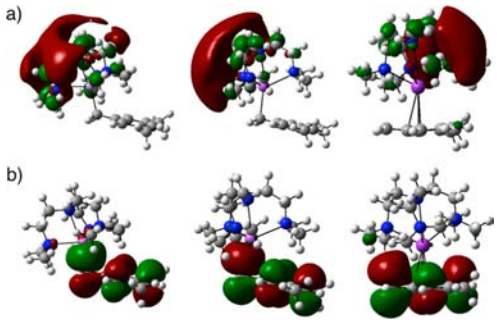

Figure 11. Frontier molecular orbitals of complexes **4** (left), **5** (center), and **6** (right); a = LUMO, b = HOMO.

at the same position for each example, specifically in these cases at the CH_2 group.

Synthesis of Heterobimetallic Complex. With this part of the study complete and given our ongoing interest in bimetallic frameworks containing alkali-metals, we contemplated what effect the use of a π-bound organo alkali-metal reagent would have. For ease of synthesis we reverted to using unsubstituted benzyl complex **3** ($PhCH_2K{\cdot}Me_6TREN$) and opted for zinc (specifically tBu_2Zn) as the second metal.[27] Complex **3** was prepared in situ in toluene,[7] and a toluene solution containing one equivalent of tBu_2Zn was added via cannula with stirring. The deep red color of the solution was seen to pale but not completely dissipate. After reducing the volume the solution was cooled to deposit X-ray quality crystals of a new complex, $tBu_2Zn(PhCH_2)K{\cdot}Me_6TREN$ (**3**·ZntBu_2), the molecular structure of which is shown in Figure 12.

This revealed that while the resulting complex is bimetallic, it does not adopt the type of motif typically seen in alkali-metal metallates. Rather than bridging between the two metals through a single point, as is the case in the related bis-TMEDA solvated sodium congener,[28] the benzyl anion acts as a dual σ/π coordinating ligand (to Zn and K respectively). Such bonding does not allow the two metals to be linked via two anionic bridges as is typically the case, although this may also in part be attributed to the monomerizing ability of Me_6TREN ligand blocking any potential ligating sites on potassium. We identified two possible ways of describing **3**·ZntBu_2, either as a cocomplexation of two neutral moieties (that is of type $[PhCH_2K{\cdot}Me_6TREN][Zn tBu_2]$ with the negative charge still delocalized in the aromatic ring) or a pseudoseparated ion pair (that is of type $[K{\cdot}Me_6TREN]^+[PhCH_2Zn tBu_2]^-$ with the negative charge relocalized on the CH_2 arm and the "solvent separated" K cation having its coordination shell completed by the aromatic system of the benzyl group in the absence of other Lewis donating solvents). To ascertain which of these descriptions was the more apt we turned to both the solid state bond parameters and solution NMR data, comparing values for this new complex with homometallic **3** (Tables 1 and 2, bond parameters in Table 1 represent the major component of one of the independent molecules within the unit cell). These suggested that it is the latter, "ate" situation, which is arising here. Primarily this is attributed to the increase in the $K{-}C_{centroid}$ distance upon addition of ZntBu_2 [c.f. 2.868(1) Å versus 2.830(1) Å in **3**], which has a concomitant effect of shortening the K—N distances (mean 2.819 Å versus 2.848 Å in **3**) since the now formally neutral aromatic ring exerts less of a pull on the cation. This distance is slightly shorter than that of another K^+-benzyl interaction [2.940(1) Å in Jones' Ga(II) complex where the potassium countercation is solvated by a gallium bound benzyl group and three molecules of diethyl ether].[29] We note at this juncture that the $K{-}C_{centroid}$ distances of the crystallographically characterized supramolecular $[K(arene)_2]^+[M(HMDS)_3]^-$ (M = Mg, arene = toluene, *o*-xylene; M = Zn, arene = *p*-xylene) are in the range 2.884—3.023 Å.[30] Further, there is a clear lengthening of the diagnostic C20—C21 bond [c.f. 1.469(5) Å versus 1.390(6) Å in **3**] consistent with relocalization of the negative charge at C21 reducing the olefinic nature of this bond. The trigonal planar environment around the zinc atom mirrors that in the related complex $tBu_2Zn(PhCH_2)Na{\cdot}2TMEDA$.[28] Our complex also bears close resemblance to the amide rich potassium zincate $[KZn(HMDS)_2(CH_2Ph)]_\infty$, formed by the synergic deprotonation of toluene by the homoleptic base $KZn(HMDS)_3$ (HMDS = 1,1,1,3,3,3-hexamethyldisilazide, $N(SiMe_3)_2^-$).[31] In this complex the zinc center is also in a distorted trigonal planar environment surrounded by the benzyl CH_2 group and two nitrogen atoms of HMDS. Potassium is π bound to the arene ring with the $K{-}C_{centroid}$ distance of 2.919 Å being marginally longer than in **3**·ZntBu_2. In the absence of neutral Lewis donors the potassium atom binds to the HMDS nitrogen atoms, with these bridging amides propagating a polymeric structure.

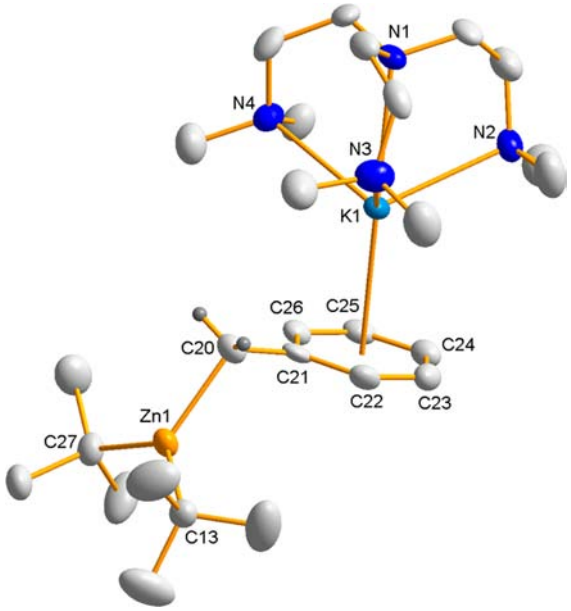

Figure 12. Molecular structure of one of the crystallographically independent molecules of $tBu_2Zn(PhCH_2)K{\cdot}Me_6TREN$ (**3**·ZntBu_2). Only one of the conformations for the disordered ligands is shown. Ellipsoids are displayed at 50% probability, and all hydrogen atoms except those of the zinc-CH_2 group are omitted for clarity.

In solution the relocalization of the negative charge at the CH_2 arm is manifested through a considerable downfield shift of the aromatic proton resonances (from 6.16, 6.56, and 5.24 ppm in **3** to 7.05, 6.85, and 6.29 ppm in **3**·ZntBu_2 for the *ortho*, *meta*, and *para* resonances, respectively) and a concomitant upfield shift of the resonance of the CH_2 arm itself from 3.21 ppm in **3** to 2.32 ppm in **3**·ZntBu_2. The $^1J_{CH}$ coupling constant is also significantly decreased from 151 Hz in the absence of tBu_2Zn to 127 Hz in its presence, clearly now more at the sp^3 hybridization end of the spectrum.

DFT Calculations. DFT calculations also supported the assignment of this complex as a potassium zincate structure. As shown in Figure 13 the calculations agree with the experimental

dx.doi.org/10.1021/ic401777x | *Inorg. Chem.* 2013, 52, 12023—12032

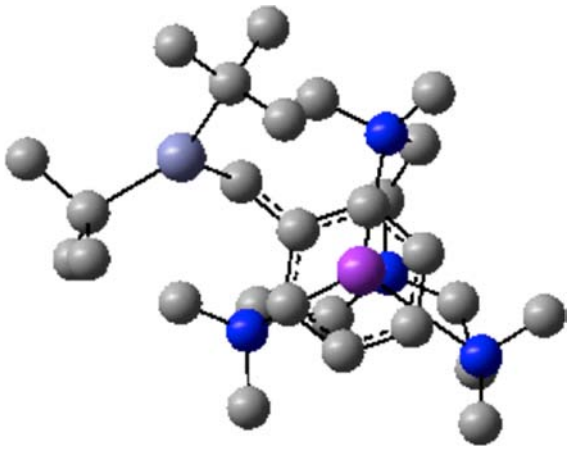

Figure 13. Optimized energy minimum structure of complex **3**·Zn*t*Bu$_2$.

finding that the minimum energy structure is a contacted bimetallic structure with the benzyl anion bridging between the *t*Bu$_2$Zn and K·Me$_6$TREN moieties in a σ/π fashion. As before, the calculations slightly overestimate the strength of the K−Ph interaction as evidenced by the C−K bond lengths (3.684 and 3.010 Å for K−CH$_2$ and K−C$_{ipso}$ respectively), with a concomitant underestimation of the K−N$_{donor}$ distances (mean 2.935 Å; mean observed in **3**·Zn*t*Bu$_2$ 2.819 Å). The calculated structure predicts a lengthening of the CH$_2$−C$_{ipso}$ bond distance (1.438 Å) with respect to the parent homometallic potassium complex (**3**) although this is predicted to be marginally shorter than the experimentally determined value of 1.469(5) Å. The effect of this is to again overestimate the CH$_2$−Zn distance by almost 0.1 Å.

CONCLUSION

In conclusion, we have now shown that alkali-metal benzyl complexes consistently display a noticeable variation in their metal-anion coordination mode depending on the identity and thus the size of the metal, altering from a strictly σ M−C bond for lithium to more of an aromatic π interaction for potassium. Such changes are clearly evident in both the solid state and also in solution, the latter case being discernible by both the change in chemical shift of the CH$_2^-$ resonance as well as the magnitude of the CH coupling constant of this functionality. This structural variation is supported by DFT calculations. Finally, when utilized as part of a bimetallic (Zn/K) system, the benzyl anion acts as a dual σ/π ligand bridging between the two metals with experimental evidence suggesting that the negative charge has been relocalized onto the CH$_2^-$ group resulting in a potassium zincate complex.

EXPERIMENTAL SECTION

General Experimental Procedures. All reactions and manipulations were carried out under a protective argon atmosphere using either standard high vacuum Schlenk techniques or an MBraun glovebox fitted with an inert gas recirculation and purification system. Hexane was dried over Na/benzophenone and freshly distilled prior to use. Mesitylene was distilled and stored over 4 Å molecular sieves. Me$_6$TREN[32] and *t*Bu$_2$Zn[33] were prepared according to literature procedures. MesNa and MesK were made from a superbasic *n*BuLi/MO*t*Bu mixture in mesitylene/hexane and collected by filtration and dried in vacuo. *n*BuLi (1.6 M in hexanes) and MO*t*Bu were purchased from Aldrich and Alfa Aesar respectively and used as received.

NMR spectra were collected on a Bruker AV400 MHz spectrometer operating at 400.13 MHz for ^{1}H, 155.47 MHz for ^{7}Li, and 100.62 MHz for ^{13}C. All ^{13}C NMR spectra were proton decoupled. Adequate elemental analyses of complexes **4**−**6** could not be obtained because of difficulty in completely removing poorly volatile mesitylene under reduced pressure coupled with acute air and moisture sensitivity. ^{1}H NMR spectra are provided in Supporting Information as alternative proof of bulk purity.

Table 4. Crystallographic Data and Refinement Details for Complexes 4−6, 3·Zn*t*Bu$_2$

	4	5	6[a]	3·Zn*t*Bu$_2$[b]
empirical formula	$C_{21}H_{41}LiN_4$	$C_{21}H_{41}NaN_4$	$C_{21}H_{41}KN_4$	$C_{27}H_{55}KN_4Zn$
mol. mass	356.52	372.57	388.68	540.22
crystal system	monoclinic	monoclinic	monoclinic	monoclinic
space group	$P2_1/n$	$P2_1/c$	$P2_1/c$	$P2_1/n$
a/Å	8.9663(2)	17.9051(11)	14.6238(11)	10.0741(2)
b/Å	14.4518(4)	8.6147(5)	9.8408(5)	38.7606(8)
c/Å	17.9228(4)	16.4284(10)	16.5207(12)	16.8231(4)
β/deg	94.940(2)	112.510(7)	91.459(8)	96.123(2)
V/Å^3	2313.79(10)	2341.0(2)	2376.7(3)	6531.6(2)
Z	4	4	4	8
measured reflections	11786	11278		35243
unique reflections	6014	6123	15223	12823
R_{int}	0.0191	0.0178		0.0410
observed rflns [$I > 2\sigma(I)$]	4570	4622	10300	9380
$2\theta_{max}$/deg	60.0	60.3	50.0	52.0
no. of parameters	250	251	244	704
GoF	1.036	1.020	1.043	1.053
R [on F, obs rflns only]	0.0496	0.0466	0.0901	0.0567
wR [on F^2, all data]	0.1321	0.1199	0.2625	0.1078
largest diff. peak/hole/e Å^{-3}	0.262/−0.209	0.267/−0.209	0.662/−0.846	0.562/−0.325

[a]Reflection data for **6** was twinned by a 180° rotation about 1 0 0. This was accounted for by reprocessing to give a SHELX hklf 5 formatted reflection file. BASF refined to 0.258. [b]Both independent TREN ligands and one of the tertiary butyl ligands were modeled as disordered, each over two sites.

dx.doi.org/10.1021/ic401777x | *Inorg. Chem.* 2013, 52, 12023−12032

$Me_2BnLi{\cdot}Me_6TREN$ (4). *n*BuLi (1.0 mL, 1.6 M in hexanes, 1.6 mmol) was added via syringe to a stirring solution of Me_6TREN (0.41 mL, 1.6 mmol) in mesitylene (5 mL), immediately changing the solution color from colorless to orange. A narrow tube containing pentane was left in the flask which was cooled to 4 °C to yield a crop of X-ray quality orange crystals. Yield 0.271 g, 47%.

^1H NMR (C_6D_6, 300 K): δ 6.47 (2H, s, *ortho* CH), 5.94 (1H, s, *para* CH), 2.37 (s, 6H, mesityl Me), 2.08 (2H, s, Li-CH_2), 1.99 (24H, broad s, Me_6TREN Me + CH_2), 1.86 ppm (6H, t, Me_6TREN CH_2).

^{13}C NMR (C_6D_6, 300 K): δ 161.1 (*ipso*), 136.6 (*meta*), 116.9 (*ortho*), 108.8 (*para*), 57.3, 51.5 (both Me_6TREN CH_2), 45.5 (Me_6TREN Me), 37.0 (Li-CH_2), 22.5 ppm (mesityl Me).

^7Li NMR (C_6D_6, 300 K): δ 0.83 ppm.

$Me_2BnNa{\cdot}Me_6TREN$ (5). MesNa (0.142 g, 1 mmol) was suspended in mesitylene (5 mL), and Me_6TREN (0.52 mL, 2 mmol) was added via syringe. After sonicating for 10 min an intensely colored solution remained which was cooled to −30 °C to yield a crop of red crystals. These were filtered, washed with cold hexane, and dried in vacuo. Yield 0.159 g, 42%.

^1H NMR (C_6D_6, 300 K): δ 6.21 (2H, s, *ortho* CH), 5.54 (1H, s, *para* CH), 2.50 (2H, s, Li-CH_2), 2.25 (s, 6H, mesityl Me), 2.02 (18H, s, Me_6TREN Me), 1.85 ppm (12H, broad s, Me_6TREN CH_2 × 2).

^{13}C NMR (C_6D_6, 300 K): δ 158.1 (*ipso*), 136.9 (*meta*), 112.0 (*ortho*), 103.9 (*para*), 57.1, 51.0 (both Me_6TREN CH_2), 45.0 (Me_6TREN Me), 41.3 (Li-CH_2), 22.6 ppm (mesityl Me).

$Me_2BnK{\cdot}Me_6TREN$ (6). This was prepared in the same manner as **5** using MesK (0.158 g, 1 mmol). Yield 0.212 g, 59%.

^1H NMR (C_6D_6, 300 K): δ 5.90 (2H, s, *ortho* CH), 4.95 (1H, s, *para* CH), 3.27 (2H, s, K-CH_2), 2.17 (6H, t, $^3J_{HH}$ = 6.0 Hz, Me_6TREN CH_2), 2.08 (6H, t, $^3J_{HH}$ = 6.0 Hz, Me_6TREN CH_2), 2.05 (18H, s, Me_6TREN Me), 2.04 ppm (s, 6H, mesityl Me).

^{13}C NMR (C_6D_6, 300 K): δ 153.5 (*ipso*), 137.7 (*meta*), 109.3 (*ortho*), 97.3 (*para*), 57.7 (Me_6TREN CH_2), 56.0 (K-CH_2), 52.7 (Me_6TREN CH_2), 45.2 (Me_6TREN Me), 22.5 ppm (mesityl Me).

***t*$Bu_2ZnBnK{\cdot}Me_6TREN$ (3·Zn*t*Bu_2).** Complex **3** was prepared in situ in toluene (5 mL) on a 1 mmol scale. *t*Bu_2Zn (0.18 g, 1 mmol) was dissolved in another flask in toluene (5 mL), and this was carefully added via cannula. The intense red color partially dissipated but did not completely disappear. The volume was slightly reduced under reduced pressure, and this was cooled to −30 °C to yield a crop of pale red crystals of X-ray quality. Yield 0.155 g, 29%.

^1H NMR (C_6D_6, 300 K): δ 7.05 (2H, d, $^3J_{HH}$ = 7.2 Hz, *ortho* CH), 6.85 (2H, t, $^3J_{HH}$ = 7.2 Hz, *meta* CH), 6.29 (1H, t, $^3J_{HH}$ = 7.2 Hz, *para* CH), 2.32 (2H, s, Zn-CH_2), 1.77−1.64 ppm (48H, m, Me_6TREN Me + CH_2 + *t*Bu).

^{13}C NMR (C_6D_6, 300 K): δ 159.0 (*ipso*), 128.9 (*meta*), 122.9 (*ortho*), 113.5 (*para*), 56.6 (Me_6TREN CH_2), 51.4 (Me_6TREN CH_2), 44.6 (Me_6TREN Me), 35.7 (CMe_3) 24.5 ppm (CMe_3). Elemental analysis calcd (%) for $C_{27}H_{55}N_4KZn$: C 60.02, H 10.26, N 10.37; found: C 59.89, H 10.42, N 10.37.

CRYSTALLOGRAPHIC ANALYSIS

Crystallographic data were collected at 123(2) K on Oxford Diffraction instrument using Mo−Kα radiation (λ = 0.71073 Å). Structures were solved using SHELXS-97,[34] and refined to convergence on F^2 against all independent reflections by the full-matrix least-squares method as implemented in SHELXL-97.[34] Selected crystallographic and refinement details are given in Table 4. CCDC-948516−948519 contain the supplementary crystallographic data for this paper. These data in cif format can be obtained free of charge from The Cambridge Crystallographic Data Centre via www.ccdc.cam.ac.uk/data_request/cif.

Theoretical Calculations. DFT calculations were performed using the Gaussian[35] computational package G03. In this series of calculations the B3LYP[36] density functional and the 6-311G(d,p)[37] basis set were used. After each geometry optimization, a frequency analysis was performed.

ASSOCIATED CONTENT

Supporting Information

Crystallographic data for complexes **4**−**6** and **3**·Zn*t*Bu_2 in CIF format, ^1H NMR spectra for complexes **4**−**6**, and optimized theoretical data for complexes **1**−**3**. This material is available free of charge via the Internet at http://pubs.acs.org.

AUTHOR INFORMATION

Corresponding Author

*E-mail: stuart.d.robertson@strath.ac.uk.

Notes

The authors declare no competing financial interest.

ACKNOWLEDGMENTS

We are grateful to the Royal Society of Edinburgh (BP Trust Fellowship to S.D.R.), the U.K. Engineering and Physical Sciences Research Council (award no. EP/F063733/1), the Royal Society (Wolfson research merit award to R.E.M.) and the European Commision (Marie-Curie Intra-European Post-doctoral Fellowship award no PIEF-2009-235173 to D.G.-V.).

REFERENCES

(1) (a) Stey, T.; Stalke, D. In *The Chemistry of Organolithium Compounds*; Rappoport, Z., Marek, I., Eds.; Wiley: Chichester, U.K., 2004; pp 47−120; (b) Gessner, V. H.; Däschlein, C.; Strohmann, C. *Chem.—Eur. J.* **2009**, *15*, 3320−3334.

(2) (a) Weiner, M.; Vogel, G.; West, R. *Inorg. Chem.* **1962**, *1*, 654−658. (b) Margerison, D.; Newport, J. P. *Trans. Faraday Soc.* **1963**, *59*, 2058−2063. (c) Lewis, H. L.; Brown, T. L. *J. Am. Chem. Soc.* **1970**, *92*, 4664−4670. (d) Thomas, R. D.; Clarke, M. T.; Jensen, R. M.; Young, T. C. *Organometallics* **1986**, *5*, 1851−1857. (e) Thomas, R. D.; Jensen, R. M.; Young, T. C. *Organometallics* **1987**, *6*, 565−571. (f) Kottke, T.; Stalke, D. *Angew. Chem., Int. Ed. Engl.* **1993**, *32*, 580−582. (g) Weiss, E. *Angew. Chem., Int. Ed. Engl.* **1993**, *32*, 1501−1523.

(3) (a) Collum, D. B. *Acc. Chem. Res.* **1993**, *26*, 227−234. (b) Bernstein, M. P.; Collum, D. B. *J. Am. Chem. Soc.* **1993**, *115*, 8008−8018. (c) Remenar, J. F.; Collum, D. B. *J. Am. Chem. Soc.* **1997**, *119*, 5573−5582.

(4) (a) For an example of Me_6TREN ligating an s-block metal in a η^3 manner see Cousins, D. M.; Davidson, M. G.; Frankis, C. J.; Garcia-Vivo, D.; Mahon, M. F. *Dalton Trans.* **2010**, *39*, 8278−8280. (b) For an example of Me_6TREN ligating a main group metal in a η^2 or η^1 manner see Cadenbach, T.; Hevia, E.; Kennedy, A. R.; Mulvey, R. E.; Pickrell, J.-A.; Robertson, S. D. *Dalton Trans.* **2012**, *41*, 10141−10144. (c) Me_6TREN was recently metallated at a terminal methyl arm in a Lu complex. See Venugopal, A.; Fegler, W.; Spaniol, T. P.; Maron, L.; Okuda, L. *J. Am. Chem. Soc.* **2011**, *133*, 17574−17577.

(5) For a review of tripodal tetraamine ligands see Blackman, A. G. *Polyhedron* **2005**, *24*, 1−39.

(6) Me_6TREN has also found use in s-block chemistry in the stabilization of unusual cations such as $[LiClLi]^+$ and $[MgHal]^+$. For the former see Kennedy, A. R.; Mulvey, R. E.; O'Hara, C. T.; Robertson, G. M.; Robertson, S. D. *Angew. Chem., Int. Ed.* **2011**, *50*, 8375−8378. For the latter see Guard, L. M.; Hazari, N. *Organometallics* **2013**, *32*, 2787−2794.

(7) Davidson, M. G.; Garcia-Vivo, D.; Kennedy, A. R.; Mulvey, R. E.; Robertson, S. D. *Chem.—Eur. J.* **2011**, *17*, 3364−3369.

(8) Hoffmann, D.; Bauer, W.; Hampel, F.; van Eikema Hommes, N. J. R.; Schleyer, P. v. R.; Otto, P.; Pieper, U.; Stalke, D.; Wright, D. S.; Snaith, R. *J. Am. Chem. Soc.* **1994**, *116*, 528−536.

(9) (a) The lithiation of mesitylene by BuLi in the presence of TMEDA has been studied previously. See Klein, J.; Medlik, A.; Meyer, A. Y. *Tetrahedron* **1976**, *32*, 51−56. (b) This was also studied in the presence of catalytic polyether alkoxides. See Kayhan, T.; Nugay, N.; Nugay, T. *Turk. J. Chem.* **2002**, *26*, 965−971.

(10) (a) Lochmann, L.; Pospišil, J.; Lim, D. *Tetrahedron Lett.* **1966**, *7*, 257−262. (b) Schlosser, M. *J. Organomet. Chem.* **1967**, *8*, 9−16. (c) Schlosser, M. *Pure Appl. Chem.* **1988**, *60*, 1627−1634. (d) Lochmann, L. *Eur. J. Inorg. Chem.* **2000**, 1115−1126.
(11) (a) Setzer, W. N.; Schleyer, P. v. R. *Adv. Organomet. Chem.* **1985**, *24*, 353−451. (b) Schade, C.; Schleyer, P. v. R. *Adv. Organomet. Chem.* **1987**, *27*, 169−278. (c) Lambert, C.; Schleyer, P. v. R. In *Methoden der Organischen Chemie (Houben-Weyl), Vol. E/19d*; Hanack, M., Ed.; Thieme: Stuttgart, Germany, 1993; pp 1−98; (d) Lambert, C.; Schleyer, P. v. R. *Angew. Chem., Int. Ed. Engl.* **1994**, *33*, 1129−1140.
(12) (a) Feil, F.; Harder, S. *Organometallics* **2000**, *19*, 5010−5015. (b) Feil, F.; Harder, S. *Organometallics* **2001**, *20*, 4616−4622.
(13) Bildmann, U. J.; Müller, G. *Organometallics* **2001**, *20*, 1689−1691.
(14) Beno, M. A.; Hope, H.; Olmstead, M. M.; Power, P. P. *Organometallics* **1985**, *4*, 2117−2121.
(15) Hübner, A.; Bernert, T.; Sänger, I.; Alig, E.; Bolte, M.; Fink, L.; Wagner, M.; Lerner, H.-W. *Dalton Trans.* **2010**, *39*, 7528−7533.
(16) (a) Davies, R. P.; Hornauer, S.; Hitchcock, P. B. *Angew. Chem., Int. Ed.* **2007**, *46*, 5191−5194. (b) Davies, R. P.; Hornauer, S.; White, A. J. P. *Chem. Commun.* **2007**, 304−306. (c) Bomparola, R.; Davies, R. P.; Hornauer, S.; White, A. J. P. *Dalton Trans.* **2009**, 1104−1106.
(17) Allen, F. H. *Acta Crystallogr.* **2002**, *A58*, 380−388.
(18) (a) Zarges, W.; Marsch, M.; Harms, K.; Boche, G. *Chem. Ber.* **1989**, *122*, 2303−2309. (b) Arnold, J.; Knapp, V.; Schmidt, J. A. R.; Shafir, A. *J. Chem. Soc., Dalton Trans.* **2002**, 3273−3274. (c) Tatic, T.; Hermann, S.; John, M.; Loquet, A.; Lange, A.; Stalke, D. *Angew. Chem., Int. Ed.* **2011**, *50*, 6666−6669.
(19) (a) Patterman, S. P.; Karle, I. L.; Stucky, G. D. *J. Am. Chem. Soc.* **1970**, *92*, 1150−1157. (b) Müller, G.; Lutz, M.; Waldkircher, M. *Acta Crystallogr.* **1996**, *C52*, 1182−1184. (c) Hage, M.; Ogle, C. A.; Rathman, T. L.; Hubbard, J. L. *Main Group Met. Chem.* **1998**, *21*, 777−782.
(20) Schade, C.; Schleyer, P. v. R.; Dietrich, H.; Mahdi, W. *J. Am. Chem. Soc.* **1986**, *108*, 2484−2485.
(21) Corbelin, S.; Lorenzen, N. P.; Kopf, J.; Weiss, E. *J. Organomet. Chem.* **1991**, *415*, 293−313.
(22) A heterometallic cyclotetramer with lithium and sodium atoms alternating in the metal positions has also been reported Baker, D. R.; Clegg, W.; Horsburgh, L.; Mulvey, R. E. *Organometallics* **1994**, *13*, 4170−4171.
(23) Kraft, S. J.; Fanwick, P. E.; Bart, S. C. *J. Am. Chem. Soc.* **2012**, *134*, 6160−6168.
(24) Moorhouse, R. S.; Moxey, G. J.; Ortu, F.; Reade, T. J.; Lewis, W.; Blake, A. J.; Kays, D. L. *Inorg. Chem.* **2013**, *52*, 2678−2683.
(25) Carpenter, J. E.; Weinhold, F. *J. Mol. Struct. (Theochem)* **1988**, *169*, 41−62.
(26) Ott, H.; Pieper, U.; Leusser, D.; Flierler, U.; Henn, J.; Stalke, D. *Angew. Chem., Int. Ed.* **2009**, *48*, 2978−2981.
(27) (a) Kondo, Y.; Shilai, M.; Uchiyama, M.; Sakamoto, T. *J. Am. Chem. Soc.* **1999**, *121*, 3539−3540. (b) Uchiyama, M.; Miyoshi, T.; Kajihara, Y.; Sakamoto, T.; Otani, Y.; Ohwada, T.; Kondo, Y. *J. Am. Chem. Soc.* **2002**, 124. (c) Hevia, E.; Honeyman, G. W.; Kennedy, A. R.; Mulvey, R. E. *J. Am. Chem. Soc.* **2005**, *127*, 13106−13107. (d) Clegg, W.; Dale, S. H.; Drummond, A. M.; Hevia, E.; Honeyman, G. W.; Mulvey, R. E. *J. Am. Chem. Soc.* **2006**, *128*, 7434−7435. (e) Uchiyama, M.; Matsumoto, Y.; Nobuto, D.; Furuyama, T.; Yamaguchi, K.; Morokuma, K. *J. Am. Chem. Soc.* **2006**, *128*, 8748−8750. (f) Clegg, W.; Dale, S. H.; Hevia, E.; Hogg, L. M.; Honeyman, G. W.; Mulvey, R. E.; O'Hara, C. T. *Angew. Chem., Int. Ed.* **2006**, *45*, 6548−6550. (g) Zn and K have also been paired together in a bimetallic amido-based framework for the generation of "inverse crowns". See Forbes, G. C.; Kennedy, A. R.; Mulvey, R. E.; Rowlings, R. B.; Clegg, W.; Liddle, S. T.; Wilson, C. C. *Chem. Commun.* **2000**, 1759−1760.
(28) Armstrong, D. R.; García-Álvarez, J.; Graham, D. V.; Honeyman, G. W.; Hevia, E.; Kennedy, A. R.; Mulvey, R. E. *Chem.—Eur. J.* **2009**, *15*, 3800−3807.
(29) Jones, C.; Mills, D. P.; Rivard, E.; Stasch, A.; Woodul, W. D. *J. Chem. Crystallogr.* **2010**, *40*, 965−969.
(30) Forbes, G. C.; Kennedy, A. R.; Mulvey, R. E.; Roberts, B. A.; Rowlings, R. B. *Organometallics* **2002**, *21*, 5115−5121.
(31) Clegg, W.; Forbes, G. C.; Kennedy, A. R.; Mulvey, R. E.; Liddle, S. T. *Chem. Commun.* **2003**, 406−407.
(32) Britovsek, G. J. P.; England, J.; White, A. J. P. *Inorg. Chem.* **2005**, *44*, 8125−8134.
(33) Andrikopoulos, P. C.; Armstrong, D. R.; Barley, H. R. L.; Clegg, W.; Dale, S. H.; Hevia, E.; Honeyman, G. W.; Kennedy, A. R.; Mulvey, R. E. *J. Am. Chem. Soc.* **2005**, *127*, 6184−6185.
(34) Sheldrick, G. M. *Acta Crystallogr.* **2007**, *A64*, 112−122.
(35) Frisch, M. J.; Trucks, G. W.; Schlegel, H. B.; Scuseria, G. E.; Robb, M. A.; Cheeseman, J. R.; Montgomery, J. A.; Jr, Vreven, T.; Kudin, K. N.; Burant, J. C.; Millam, J. M.; Iyengar, S. S.; Tomasi, V.; Barone, B.; Mennucci, B.; Cossi, M.; Scalmani, G.; Rega, N.; Petersson, G. A.; Nakatsuji, H.; Hada, M.; Ehara, M.; Toyota, K.; Fukuda, R.; Hasegawa, J.; Ishida, M.; Nakajima, T.; Honda, Y.; Kitao, O.; Nakai, H.; Klene, M.; Li, X.; Knox, J. E.; Hratchian, H. P.; Cross, J. B.; Bakken, V.; Adamo, C.; Jaramillo, J.; Gomperts, R.; Stratmann, R. E.; Yazyev, O.; Austin, A. J.; Cammi, R.; Pomelli, C.; Ochterski, J. W.; Ayala, P. Y.; Morokuma, K.; Voth, G. A.; Salvador, P.; Dannenberg, J. J.; Zakrzewski, V. G.; Dapprich, S.; Daniels, A. D.; Strain, M. C.; Farkas, O.; Malick, D. K.; Rabuck, A. D.; Raghavachari, K.; Foresman, J. B.; Ortiz, J. V.; Cui, Q. B.; Baboul, A. G.; Clifford, S.; Cioslowski, J.; Stefanov, B. B.; Liu, G.; Liashenko, A.; Piskorz, P.; Komaromi, I.; Martin, R. L.; Fox, D. J.; Keith, T.; M. A. Al-Laham, Peng, C. Y.; Nanayakkara, A.; Challacombe, M.; Gill, P. M. W.; Johnson, B.; Chen, W.; Wong, M. W.; Gonzalez, C.; Pople, J. A. *Gaussian03*, Revision C.02; Gaussian, Inc.: Wallingford, CT, 2004.
(36) (a) Kohn, W.; Becke, A. D.; Parr, R. G. *J. Phys. Chem.* **1996**, *100*, 12974−12980. (b) Becke, A. D. *Phys. Rev. A* **1988**, *38*, 3098−3100.
(37) (a) McLean, A. D.; Chandler, G. S. *J. Chem. Phys.* **1980**, *72*, 5639−5648. (b) Krishnan, R.; Binkley, J. S.; Seeger, R.; Pople, J. A. *J. Chem. Phys.* **1980**, *72*, 650−654.